

Synthesis of Multifunctional Nanocomposites Based on Highly Ordered Mesoporous Silica

Zhengyang Zhou, Shenmin Zhu,* and Di Zhang

State Key Laboratory of Metal Matrix Composites, Shanghai Jiao Tong University (SJTU),
1954 Huashan Road, Shanghai 200030, P. R. China

(Received March 20, 2006; CL-060335; E-mail: smzhu@sjtu.edu.cn)

A synthetic method for the preparation of multifunctional nanocomposites with well-defined mesoporosity based on highly ordered mesoporous silica SBA-15 was presented. Thermoresponsive PNIPAA and magnetic nanoparticles Fe_2O_3 were inserted into the pore channels of SBA-15 combining nanocasting method with ultrasonic chemistry.

Highly ordered mesoporous silica SBA-15 has attracted much attention since it was first reported¹ in 1998. Many efforts have been devoted to synthesize functional nanocomposites by using it as hosts for inclusion compounds of inorganic nanoparticles^{2,3} or polymers.⁴ Generally, inorganic precursors can be incorporated into the channels of mesoporous silica by ion exchange, wetness impregnation, chemical vapor infiltration, as well as cocondensation.⁵ Meanwhile, many novel organic-inorganic nanocomposites have been prepared through sorption, postpolymerization modification, and in situ polymerization⁵ in the pore channels of mesoporous silica. Mesoporous silica materials could be more applicable if they are functionalized with organic or inorganic materials.

To the best of our knowledge, no research has been directed toward the preparation of nanocomposite based on mesoporous silica that includes both inorganic and organic components inside their channels. We report herein a multifunctional nanocomposite based on SBA-15 with both thermoresponsive poly(*N*-isopropylacrylamide) (PNIPAA) and nanomagnetic particles Fe_2O_3 inside the mesopores. Multifunctional nanocomposites with well-defined mesoporosity play an important role in many fields, such as label and controlled drug delivery.

The concept and the fabrication procedure of the proposed multifunctional nanocomposites are schematically illustrated in Figure 1. The first step in the procedure was to functionalize SBA-15 with the amino group⁶ of 3-aminopropyltriethoxysilane (APTES) to ensure the absorption of NIPAA monomer in the

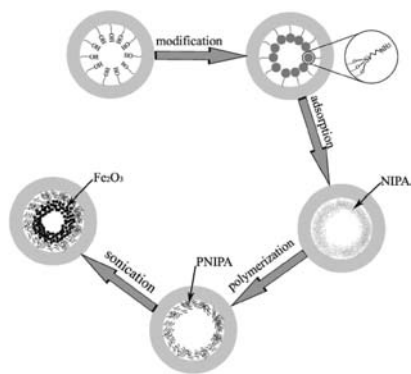


Figure 1. Schematic illustration for fabrication of the multifunctional nanocomposites with well-defined mesoporosity.

internal surface of SBA-15, the sample is thus obtained as m-SBA-15. Then, 0.2 g of NIPAA monomer, 0.003 g of azobisisobutyronitrile and 0.02 g of *N,N'*-methylene bisacrylamide were absorbed in the pore channels of 0.3 g of m-SBA-15, and PNIPAA nanocasting SBA-15 can be obtained via in situ free-radical polymerization under nitrogen, the powder thus prepared was designated as SBA-PNIPAA. Next, 0.3 g of pre-prepared SBA-PNIPAA, 0.5 mL of iron pentacarbonyl, and 30 mL of decalin were mixed together, and then the mixture was irradiated with a high-intensity ultrasonic horn (Ti-horn, 20 kHz, 100 W cm⁻²) under argon atmospheres at 0 °C for 3 h,⁷ resulting in the materials of multifunctional nanocomposites SBA-PNIPAA- Fe_2O_3 . Nanocasting of polymer inside the pores was characterized through N_2 adsorption/desorption. The incorporation of Fe_2O_3 inside the channels of SBA-15 was detected directly from TEM images. As is well known, PNIPAA is one of the most typical thermo-responsive polymers. It exhibits a reversible hydration-dehydration change in response to temperature around its lower critical solution temperature (LCST) of 32 °C.⁸ The novelty of the method lies in combination of ultrasonication with nanocasting method in realizing multifunctional nanocomposites with well-defined mesoporosity, which has a potential application in drug delivery system.

Prominent differences are observed when the polymers are synthesized and Fe_2O_3 subsequently loaded within amino-modified SBA-15, as evidenced by powder X-ray diffraction (XRD) in Figure 2.

A well-resolved peak together with two small peaks can be indexed as the diffraction planes of (100), (110), and (200) due to the hexagonal array of mesopores for the sample of m-SBA-15 (unit length = 7.4 nm). Only one peak was detected distinctly for both SBA-PNIPAA and SBA-PNIPAA- Fe_2O_3 , relating to the well-ordered mesoporous structures disturbed slightly after polymerization of NIPAA and loading Fe_2O_3 nanoparticles. In comparison with m-SBA-15, a relatively large shift of (100) reflection to a low angle was observed for the product of SBA-PNIPAA (unit length = 9.1 nm), contributing to the thicker

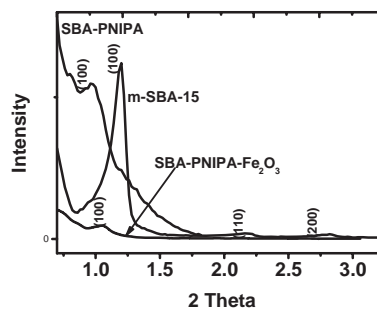


Figure 2. Powder X-ray diffraction patterns of samples m-SBA-15, SBA-PNIPAA, and SBA-PNIPAA- Fe_2O_3 .

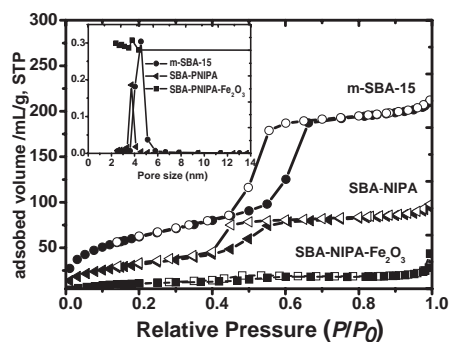


Figure 3. N₂ adsorption-desorption isotherms and pore size distribution (inset) for all samples.

Table 1. Textural parameters of various samples

Sample	SBET/m ² g ⁻¹	Pore size/nm	V _p /cm ³ g ⁻¹
m-SBA-15	229	4.5	0.33
SBA-PNIPA	146	3.7	0.14
SBA-PNIPA-Fe ₂ O ₃	42	3.7	0.07

mesopore walls due to polymerized of PNIPA inside mesopores of m-SBA-15.⁹ A reduction of scattering contrast between the pores and the framework can be attributed to the pore filling effect of PNIPA and Fe₂O₃ for the resultant SBA-PNIPA and SBA-PNIPA-Fe₂O₃ as described by others.¹⁰

Quantitative determination of organic content by thermogravimetric analysis (TGA) shows that around 57 wt % of PNIPA was contained in SBA-PNIPA. To ascertain the positions of the filling materials PNIPA and Fe₂O₃, N₂ adsorption/desorption measurements were undertaken (Figure 3). The textural parameters of the samples are summarized in Table 1.

The surface areas were found to decrease from 299 to 146 and 42 m² g⁻¹ corresponding to m-SBA-15, SBA-PNIPA, and SBA-PNIPA-Fe₂O₃, respectively. Meanwhile, the mesopore size of SBA-PNIPA was detected to reduce from 4.5 to 3.7 nm comparing with m-SBA-15 shown in Figure 3 inset. The thick wall (=5.4 nm) together with the small pores result in the relatively low surface area (146 m² g⁻¹) with respect to m-SBA-15 (229 m² g⁻¹, wall size = 2.8 nm). In other words, the thicker wall is due to the polymerization of PNIPA inside the pores. This leads to the conclusion that PNIPA has coated inside the mesopores of SBA-15. No distinct hysteresis was demonstrated for the product SBA-PNIPA-Fe₂O₃, and this together with the great decrease of pore volume from 0.14 to 0.07 cm³ g⁻¹ suggested the formation of nanoparticles Fe₂O₃ inside the mesopores.

TEM micrographs were employed to further confirm the existence of Fe₂O₃ inside SBA-15. Depicted in Figure 4, one can distinguish the formation of Fe₂O₃ around the hexagonal pores. The black stripes are the Fe₂O₃ along and perpendicular to the direction of the hexagonal pore arrangement in the SBA-PNIPA-Fe₂O₃ sample. Energy dispersive X-ray spectroscopy (EDX) measurement reveals the existence of Fe, O, N, C, and Si in the composite of SBA-PNIPA-Fe₂O₃ (not shown).

Differential scanning calorimetric measurements (DSC) were carried out to further investigate the thermal responsive

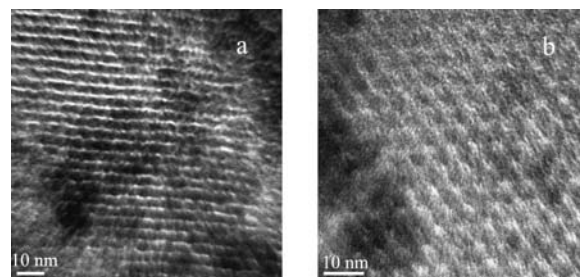


Figure 4. TEM images of sample SBA-PNIPA-Fe₂O₃.

ability of PNIPA inside the channels of SBA-15. Interestingly, the LCST was found only to be 21 °C. The reason may possibly be explained by quantum confined effect: on account of the molecular chains confined in the SBA-15 nanochannels, the competition between intermolecular and intramolecular hydrogen-bonding and hydrophilic-hydrophobic interaction can be influenced greatly.¹¹ As a comparison, a sample was prepared with PNIPA polymerized outside SBA-15 channels. The sample thus synthesized was discovered to possess a normal LCST of 32 °C. This further verified the successful synthesis of thermally responsive materials inside SBA-15.

In summary, a novel synthetic method for the preparation of multifunctional nanocomposites based on mesoporous silica SBA-15 was presented. Thermoresponsive PNIPA and magnetic nanoparticles Fe₂O₃ were inserted into the pore channels of SBA-15 through nanocasting method and ultrasonication. The special structure and multifunctional properties enable it potential applications in drug delivery, catalyst, and biosensor.

Financial support of NSF of China (Grant No. 50573013), Shanghai Science and Technology Foundation (05ZR1077) are gratefully acknowledged. The authors thank SJTU Instrument Analysis Center for the measurements.

References

- 1 D. Zhao, J. Feng, Q. Huo, N. Melosh, G. H. Frdrickson, B. F. Chmelka, G. D. Stuck, *Science* **1998**, 279, 548.
- 2 J. Zhu, Z. Konya, V. F. Puentes, I. Kiricsi, C. X. Miao, J. W. Ager, A. P. Alivisatos, G. A. Somorjai, *Langmuir* **2003**, 19, 4396.
- 3 C. Garcia, Y. Zhang, F. DiSalvo, U. Wiesner, *Angew. Chem., Int. Ed.* **2003**, 42, 1526.
- 4 M. Chio, F. Kleitz, D. Liu, H. Y. Lee, W.-S. Ahn, R. Ryoo, *J. Am. Chem. Soc.* **2005**, 127, 1924.
- 5 J. L. Shi, Z. L. Hua, L. X. Zhang, *J. Mater. Chem.* **2004**, 14, 795.
- 6 Y. Shan, L. Gao, *Mater. Chem. Phys.* **2005**, 89, 412.
- 7 Z. Y. Zhong, Y. M. Zhao, Y. Koltypin, A. Gedanken, *J. Mater. Chem.* **1998**, 8, 2167.
- 8 M. Heskins, J. E. Guillet, *J. Macromol. Sci., Chem.* **1968**, A2, 1441.
- 9 J. Sauer, F. Marlow, F. Schuth, *Phys. Chem. Chem. Phys.* **2001**, 3, 5579.
- 10 R. Ryoo, J. M. Kim, C. H. Ko, C. H. Shi, *J. Phys. Chem.* **1996**, 100, 17718.
- 11 C. Lin, L. Z. Meng, X.-J. Lu, Z. Q. Wu, L. F. Zhang, Y. B. He, *Macromol. Chem. Phys.* **2005**, 206, 1870.